

## EVALUATION OF THE SURFACE PROPERTIES OF ILLINOIS BASIN COALS

I. Demir<sup>1</sup>, A. A. Lizzio<sup>1</sup>, E. L. Fuller<sup>2</sup>, and R. D. Harvey<sup>1</sup>

<sup>1</sup>Illinois State Geological Survey, 615 E. Peabody Drive, Champaign, IL 61820. <sup>2</sup>Oak Ridge National Laboratory, PO Box 2008, MS-6088, 1 Bethel Valley Road, Oak Ridge, TN 37831

Keywords: coal, surface area, diffuse reflectance infrared spectroscopy

### INTRODUCTION

The surface properties of coal, such as surface area, pore volume and surface chemical structure, affect the physical-chemical behavior of coal in many coal conversion and cleaning processes. Knowledge of the surface area and porosity of a given coal is of major importance in understanding the mass transport phenomena that govern its physical-chemical behavior. For example, Mahajan and Walker [1] pointed out that the amount and ease of extraction of coal-bed methane are controlled by the porosity and pore size distribution of the coal. The porosity of coal affects its specific gravity, which is critical in those coal preparation processes that take advantage of density differences between coal and mineral matter. In coal conversion (e.g., gasification), the transport of reactants to the internal coal surface and the escape of product molecules from the pores are significantly influenced by the pore structure. Surface area and porosity data can be especially useful for removal of organic sulfur from coal. Organic sulfur occurs in coal as part of both aromatic and aliphatic functional groups and as thioether bridges [2,3]; that is, most of the organic sulfur appears to be located on or near the micropore walls. An important limiting factor for removal of organic sulfur may be the diffusion of reacting agents into and product molecules out of the micropores. Knowledge of the pore structure of the coal precursor can also be helpful in predicting the type of porosity that may develop and, hence, in assessing the suitability of the coal for the production of activated carbons, carbon molecular sieves, etc.

Interpretations of data on surface area and porosity of coal differ due to the physical and chemical complexity of coal. Gregg and Sing [4] reviewed the use of adsorption methods for the determination of surface area and pore size distribution of porous solids. Fuller [5] suggested that accessibility (to adsorbates) is probably a better term to define the surface area and pore structure of coal. Marsh [6] stated that the concept of a "real" or "true" physical surface area does not exist for microporous coals and carbons and recommends the use of the "equivalent" surface area, i.e., the value of surface area which the adsorbent exhibits under the experimental conditions used. The commonly applied theoretical equations used to interpret adsorption isotherms include those of Langmuir, Brauner-Emmett-Teller (BET), Dubinin-Radushkevich (DR), and Dubinin-Astakhov (DA). The Langmuir and BET equations supposedly predict monolayer coverage by the adsorbate in porosity on external surfaces, from which a surface area can be calculated. The other two equations essentially are applied to CO<sub>2</sub> adsorption to predict the micropore volume that can then be multiplied by the cross-sectional area of the CO<sub>2</sub> molecule to calculate the surface area. Because a large percentage of the coal porosity is in micropores (<20 Å in diameter), micropore surface area very closely approximates the total surface area [7].

Mercury porosimetry is another technique that is used to determine surface area and pore volume of coal. The mercury porosimetry technique is based on measuring the amount of mercury penetration into pores as a function of applied pressure. Although coals are aperture-cavity type materials [1,8], the mercury porosimetry computations treat pores as cylindrically shaped. Such a simplification is generally accepted for treating what, otherwise, would be a complex problem. Mercury porosimetry yields useful data on large pores, but measurements of smaller pores (obtained at high pressures) are questionable because the compressibility of coal results in particle breakdown and/or enlargement of some pores at the expense of others.

In short, the surface area and pore volume of a microporous solid, such as coal, depend on how they are measured and how the adsorption or intrusion data are interpreted. If all conditions are specified, data on the surface area and pore volume of coal have value and application, especially for comparing the physical-chemical behavior of one coal to that of another.

Oxidation of coal samples can significantly change their porosity and surface area. For example, Kaji et al. [9] showed that the extent of low temperature (30-180°C)

oxidation correlated negatively with internal surface area of pores  $>100 \text{ \AA}$  in diameter for five coals that ranged in rank from subbituminous to anthracite. The surface chemical structure of coal can be delineated using diffuse reflectance infrared spectroscopy (DRIS) [10-12]. The DRIS technique can also be used to monitor changes in the surface chemical structure of coal during oxidation processes [13-15].

The goal of this study was to establish a data base for surface properties of the coals in the Illinois Basin Coal Sample Program (IBCSP) to aid coal scientists and engineers in the research and development of improved processes for desulfurization and increased utilization of Illinois Basin coals. Surface area and pore volume distributions and surface chemical structure of eight IBCSP coals were determined in both a (relatively) unoxidized and oxidized state. Statistical relationships among these surface properties and other available characterization data on these coals were also determined and evaluated.

## EXPERIMENTAL

### Samples

Eight of the IBCSP coals were obtained in a fresh state, i.e., with minimum prior exposure to air (Table 1). After their removal from the IBCSP storage barrels, a 750 g representative split of each coal (except IBC-108) was placed in a rod mill, purged with argon gas, and dry-ground for 30 minutes to reduce the particle size to  $<100$  mesh; the IBC-108 coal is supplied by the IBCSP only in micronized form ( $<400$  mesh). An analysis of the ground samples with a Microtrac particle size analyzer indicated that the particle size of each was reduced to about 90%  $<100$  mesh ( $<149 \mu\text{m}$ ) with a mean volume size diameter ranging from 38 to 60  $\mu\text{m}$ . A split of each ground sample was analyzed for surface properties in the fresh state. Another split of each sample was exposed to air oxidation at room temperature for two months and then analyzed similarly to investigate the effect of this mild oxidation on the surface properties of the coals. The analytical methods used to determine the surface properties of the samples are briefly described below.

### Gas Adsorption

The samples were analyzed on a Quantachrome Autosorb-1 gas sorption system to obtain  $\text{CO}_2$  and  $\text{N}_2$  adsorption isotherms at 273 and 77 K, respectively. Surface areas were computed from the analysis of  $\text{N}_2$  and  $\text{CO}_2$  adsorption isotherms using the BET and DR equations, respectively. Molecular cross-sectional areas used in the computations were 18.7  $\text{\AA}^2$  for  $\text{CO}_2$  and 16.2  $\text{\AA}^2$  for  $\text{N}_2$ . The linear plots required for the BET and DR equations were obtained at relative pressure ( $P/P_0$ ) ranges of 0.05 to 0.2 and 0.001 to 0.01, respectively. The surface area and pore volume distributions for the portion of the micropores penetrated by  $\text{N}_2$  (5 to 20  $\text{\AA}$  diameter) and for mesopores (20 to 500  $\text{\AA}$  diameter) were calculated from  $\text{N}_2$  adsorption data using the deBoer t-equation and the Barret-Joyner-Halenda (BJH) method [16]. The total pore volume for pores 5 to about 1800  $\text{\AA}$  in diameter was determined from the amount of  $\text{N}_2$  adsorbed at 77 K at a relative pressure of 0.99.

### Mercury Porosimetry

The samples were analyzed on a Micromeritics Autopore II mercury intrusion porosimeter in the pressure range of 5 to 60,000 psia that produced surface area and pore volume distributions for pores with diameters of 30 to 10,000  $\text{\AA}$ . A surface tension of 485 dynes/cm and a contact angle of 130° for mercury were used in the computations. Although, based on the particle size analyses of the samples, the 10,000  $\text{\AA}$  (1  $\mu\text{m}$ ) dimension was estimated to be the size of the smallest particles and thus the lower limit of the interparticle space, the presence of some interparticle space with diameters smaller than 10,000  $\text{\AA}$  cannot be ruled out.

### Diffuse Reflectance Infrared Spectroscopy (DRIS)

The ground coal samples were analyzed on a computer-controlled DRIS instrument (Digilab Model 40 with diffuse reflectance attachment) for their infrared spectra. Many (5,000 to 20,000) interferograms were acquired and averaged to achieve a high signal to noise ratio. Mechanical and mathematical smoothing were not used to avoid band distortion.

## RESULTS AND DISCUSSION

### Surface Area and Pore Volume

**Fresh Samples.** Table 2 shows that the  $\text{N}_2$ -BET surface areas of the fresh samples ranged from 4 to 53  $\text{m}^2/\text{g}$  which were less than their corresponding  $\text{CO}_2$ -DR surface areas (112-152  $\text{m}^2/\text{g}$ ). This difference can be attributed to the lower activated diffusion rate of  $\text{N}_2$  in the micropores at 77 K compared to that of  $\text{CO}_2$  at 273 K [17]. It is

generally assumed that the  $N_2$ -BET surface area represents the area contained in all pores having a diameter greater than about 5 Å [18], and the  $CO_2$ -DR surface area represents the entire surface area of coal [1,4,18] that, in practice, is referred to the surface area in all pores with diameters greater than 3.5 Å. In addition,  $CO_2$  is likely to penetrate both open and closed pores through imbibition [19], thus yielding higher surface areas than  $N_2$ .

Gumkowski et al. [20] reported a  $N_2$  surface area of 23.5  $m^2/g$  for a sample that was obtained from the same mine as IBC-105 coal, consistent with the result on IBC-105 coal (Table 2). Machin et al. [21] reported  $N_2$ -BET surface areas ranging from 1.8 to 91.8  $m^2/g$  for sixteen high volatile A (hVA) and high volatile B (hVB) bituminous coals from the Illinois Basin. Thomas and Damberger [22] measured  $N_2$ -BET surface areas of 1.8 to 99  $m^2/g$  for three samples and  $CO_2$ -BET surface areas of 46 to 292  $m^2/g$  for forty samples from Illinois mines; hVA bituminous coals had the lowest and hVC bituminous coals the highest  $CO_2$ -BET surface areas. Mercury porosimetry measurements reported by Thomas and Damberger revealed that the hVC coals contained a large number of pores with diameters of 90 to 220 Å whereas relatively few pores in hVA coals were greater than 35 Å. Previous studies [21-23] indicated that, in a given coal, vitrinite macerals have a higher microporosity and surface area than inertinite macerals. Gan et al. [18] determined  $N_2$ -BET (77 K) and  $CO_2$ -BET (298 K) surface areas of twenty six coals from various locations in the United States. One of their samples (PSOC-22) was similar to the IBC-101 coal and another one (PSOC-24) to IBC-102 coal in terms of their seam of origin and carbon content. They reported  $N_2$ -BET and  $CO_2$ -BET surface areas of 88 and 169  $m^2/g$ , respectively, for PSOC-22. For sample PSOC-24, they reported a  $N_2$ -BET surface area of 2.2  $m^2/g$  and a  $CO_2$ -BET surface area of 228  $m^2/g$ . These values are different from those for IBC-101 and IBC-102 coals reported in Table 2. This discrepancy can be attributed to differences in the methods used and variations in the properties of the samples, again demonstrating that surface area data on coals depend on experimental conditions and/or can vary from sample to sample within the same rank and seam.

Most of the  $N_2$  surface area of the samples was assigned to mesopores (20-500 Å in diameter) (Table 2). Pores with diameters between 5 and 20 Å were referred to here as " $N_2$ -micropores". A very small or insignificant  $N_2$ -micropore surface area suggested that either  $N_2$  penetration into 5 to 20 Å diameter pores was physically limited or that most of the micropore surface area was derived from pores smaller than 5 Å in diameter that were penetrated by  $CO_2$  but not by  $N_2$ .

The  $CO_2$  surface area of the IBC-101 coal was the lowest and that of the IBC-109 coal highest among the samples (Table 2). The  $N_2$  surface areas (mostly in mesopores) of IBC-101, IBC-102, and IBC-107 coals were considerably higher than those of the other four coals (Table 2). The IBC-103 coal, the highest rank and lowest equilibrium moisture coal (Table 1), had the lowest  $N_2$  surface area among the eight coals (Table 2). Surface area distributions of the coals showed considerable variation from one coal to another, as illustrated by three examples in Figure 1. Surface area distributions in Figure 1 were calculated assuming average diameter of a cylindrical pore filled with  $N_2$  in each pore size range and, therefore, the cumulative area was different from  $N_2$ -BET surface area which was based on monolayer coverage of entire surface. Most of the  $N_2$  pore volume was derived from mesopores and macropores (Table 2). The  $N_2$  pore volume of the fresh samples had a five-fold range (0.017 to 0.083  $cm^3/g$ ), with sample IBC-103 having the lowest value.

The above discussions regarding differences in surface area and porosity among the samples may have implications for the response of these coals to coal conversion and cleaning processes. For example, the IBC-103 coal, which has the second highest micropore surface area (as indicated by high  $CO_2$  surface area), may resist chemical desulfurization more than the other coals because its relatively low mesopore surface area and pore volume would limit the diffusion of reacting agents into and product molecules out of the micropores. The opposite can be said for coals IBC-101 and IBC-102 which have relatively high ratios of mesopore to micropore surface areas. Raw coals possess molecular sieving capabilities to some extent, but because of their low adsorption capacity they have limited application. The IBC-103 coal could possibly be used as a "primitive" carbon molecular sieve without charring since carbons which exhibit large differences in  $N_2$  and  $CO_2$  surface areas are known to make good sieves for separation of  $O_2$  and  $N_2$  [24].

Like the gas adsorption data, mercury porosimetry measurements showed that surface area and pore volume distributions vary significantly among the samples (Table 3).

Surface areas of mesopores derived from mercury porosimetry for coals IBC-101, IBC-102, and IBC-107 were higher than those of the other four coals (Table 3), consistent with the  $N_2$  adsorption data (Table 2). However, according to the mercury porosimetry results (Table 3), the fresh coal IBC-106 had the lowest mesopore surface area among the eight coals, inconsistent with the  $N_2$  adsorption data (Table 2). Mercury porosimetry indicated higher surface areas and pore volumes than the  $N_2$  adsorption method for similar pore size ranges (Figs. 2 and 3). Mercury intrusion, even at these relatively low intrusion pressures (1000-3600 psia), probably compressed the coal and, accordingly, enlarged the mesopores at the expense of micropores. Different results from the two techniques also could arise from the different equations and assumptions for each technique.

Because mineral matter comprises only a small portion of the samples and has only very small surface area and porosity, the measured surface areas and pore volumes are mostly derived from the organic matter portion of the coal. Although adjusting the values in Tables 2 and 3 for mineral matter would increase the surface areas of all the samples, the interpretations made above would not change.

**Effect of Room Temperature Air-Oxidation.** The  $CO_2$  surface area of all coals, except IBC-103, increased somewhat as a result of exposure to air at room temperature for a two-month period with IBC-101 coal showing the greatest increase (Fig. 4). Although some of these changes were within the analytical error (standard error = 3%), a consistent change in only one direction suggests a real trend. The increased  $CO_2$  surface area with air-oxidation is consistent with a controversial mechanism discussed in the literature [19]; the adsorption of  $CO_2$  increases, at least slightly, with increased oxygen functional groups present on the coal surface.

It is interesting to note that for five of the samples, the macropore volume in pores  $>1800 \text{ \AA}$  decreased as a result of the exposure of the coals to room temperature air oxidation (Table 5). Although the cause of this observation cannot be determined from the present data, the oxidation and resulting increased molar volume of mineral matter disseminated in the macropores is one of the possibilities. For example, the respective molar volumes of gypsum and hematite, two oxidation products of pyrite, are 3.1 and 1.3 times that of pyrite. The unusually high pore volume for coal IBC-108 (Table 3, Fig. 3) was due to the fine particle size of this sample ( $<400 \text{ mesh}$ ) that caused some of the interparticle space in the sample to be counted as pore space.

#### **Statistical Analyses**

Correlation coefficients and regression plots were determined for the data on surface area, pore volume, and other coal characteristics. Because coal IBC-108 had been provided in slurry form and processed differently from the rest of the samples, it was excluded from the statistical analyses.

Figure 5 and Table 4 show that the  $CO_2$  surface area correlated positively with apparent rank, i.e., the  $CO_2$  surface area tended to increase with increasing heating value and decrease with increasing volatile matter and equilibrium moisture of the coals. The observed positive correlation between apparent rank and  $CO_2$  surface area was not consistent with the general trend observed by Thomas and Damberger [22] for coals of similar carbon content. This inconsistency could be due to the fact that they used a different gas adsorption temperature (196 K vs 273 K) and a different equation (BET vs DR) to compute the  $CO_2$  surface area. The strong negative correlation between the  $CO_2$  surface area and organic sulfur (Table 4) is not meaningful in this case because high rank (high  $CO_2$  surface area) and low rank (low  $CO_2$  surface area) coals in the IBCSP originated from low-sulfur and high-sulfur mines, respectively. In contrast to the  $CO_2$  surface area,  $N_2$  surface area (mostly in mesopores) correlated negatively with apparent rank, i.e., it tended to decrease with increasing heating value (Fig. 5) and increase with increasing equilibrium moisture and volatile matter (Table 4).

#### **Surface Chemical Structure**

**Fresh Samples.** The DRIS spectra of all eight coals were found to be similar. An example of the DRIS spectra is shown in Figure 6. The sloping background curve in Figure 6 (dashed line along the lower portion of each spectrum) is a direct result of the physical scattering of the electromagnetic radiation from the coal particles. Clays in the samples gave rise to two sets of bands (Fig. 6). The hydroxyls of clays are only weakly hydrogen (H) bonded and have two vibrational bands between 3600 and 3650  $cm^{-1}$ . The second clay band set includes three characteristic bands that are due

to lattice modes of vibration at low wave numbers.

A number of hydroxyl entities (alcoholic, acidic, phenolic, aldehydic, etc.) within the organic substrate involve H bonds of various strengths and are indicated by the large absorption band envelope from 3600 to 2000  $\text{cm}^{-1}$  (Fig. 6). There is evidence of some preferential modes of vibration prevailed as noted in the maxima and inflection points of the DRIS spectra. Superimposed upon the hydroxyl band envelope is the composite envelope for the various organic hydrocarbons. The two envelopes can be analyzed independently if one assumes a linear baseline. A scaled-up version of the hydroxyl band envelope of Figure 6 (truncated by the uppermost dashed line as shown in the figure) is shown in Figure 7. Deconvolution of the hydroxyl band reveals five species with increasing H bond strengths in the sequence of 3547, 3399, 3314, 3020, and 2565  $\text{cm}^{-1}$ .

The composite envelope of the various organic hydrocarbons superimposed on the hydroxyl band envelope (Fig. 6) can be deconvolved into six components (Fig. 8), and summation curve was barely distinguishable from the parent envelope. The unsaturated hydrocarbon bands (olefinic and aromatic) predictably occur above 3000  $\text{cm}^{-1}$ , and the four bands characteristic of aliphatic modes (CH<sub>2</sub> and CH<sub>3</sub> groups) below 3000  $\text{cm}^{-1}$ . A small aldehyde (-C=O) C-H vibration band occur at 2727  $\text{cm}^{-1}$  (Fig. 6).

The absorption bands due to oxygen functional groups occur mostly in the 1900 to 1400  $\text{cm}^{-1}$  region. The presence of carbonyls is indicated by the peak at 1700  $\text{cm}^{-1}$  (Fig. 6). The absorption band below 1600  $\text{cm}^{-1}$  is due to the bending modes of vibration of the respective entities in the organic substrate. The large peak at 1600  $\text{cm}^{-1}$  is present for virtually all conjugated aromatic structures, especially if they are oxygenated to some degree. The complex, broad feature at 1100 to 1400  $\text{cm}^{-1}$  is due to the overlap of a several bending mode bands associated with the chain and ring elements in the organic matrix.

**Effect of Room Temperature Air Oxidation on Surface Chemical Structure.** The exposure of the eight IBCSP coals to air at room temperature for a 2-month period did not cause any noticeable change in their DRIS spectra. An example of the DRIS spectra of the coals exposed to the room temperature air oxidation is shown in Figure 9. The interpretation of this DRIS spectrum is similar to that of a fresh sample. As in the case of fresh samples, oxygen insertion processes formed bands that appear as shoulders (inflections) on the side of the strong polynuclear aromatic peak noted as the carbonyl band (Fig. 9). Figure 10 shows the deconvolution of the carbonyl envelope. Aldehyde carbonyls show bands centered at 1664  $\text{cm}^{-1}$ , and carboxylic acids give rise to absorption peaks centered at 1703 and 1712  $\text{cm}^{-1}$ . The band centered at 1886  $\text{cm}^{-1}$  is caused by a very highly oxidized state, probably aromatic anhydrides and/or aromatic carbonates. However, examination of the DRIS spectra for fresh samples (Fig. 6) shows similar signals for the oxygen functional groups already present in coal.

The surface area and pore volume data suggested that a small amount of oxidation took place upon exposure of the coals to room temperature air for a two-month period. Because coal surface is expected to adsorb a significant amount of oxygen within a relatively short period of time upon exposure to air [25], the surfaces of the fresh IBC coals were probably already oxidized during their collection in the field. During the two-month oxidation period, it is likely that the interior of the particles of the IBC coals became progressively oxidized. The oxidation that took place in the interior of the particles apparently was not detected by DRIS, which is a surface, not bulk analysis, technique. Some additional surface oxidation that might have taken place during the two-month oxidation period was apparently not significant enough to be detected by the DRIS technique. Comparing this study to past studies indicates that DRIS spectra would be affected only by oxidation processes that are more rigorous (longer exposure times and/or higher exposure temperatures) than those used for this study. Clemens et al. [14] monitored changes in surfaces of dried New Zealand coals as a result of exposure to oxygen or air at 30 to 180°C and concluded that the reactivity responsible for self-heating of these coals involved exothermic formation of hydroperoxides followed by their decomposition into carboxylic acid/aldehyde species. Pisupati and Scaroni [15] reported on the compositional and structural changes of selected bituminous coals during natural weathering and laboratory oxidation at 200 °C. They observed high concentrations of carboxylic acid and ketonic groups and reduced aliphatic hydrocarbon groups in most of their outcrop samples, and formation of ester groups in laboratory-oxidized samples, relative to those in fresh samples.

**REFERENCES**

1. Mahajan, O. P. and Walker, P. L., In: Analytical Methods for Coal and Coal Products, C. Karr (ed.), Academic Press, NY (1978).
2. Attar, A., and Dupuis, F., In: Coal Structure, M. L. Gorbaty and K. Ouchi (eds.), Advances in Chem. Ser., 192, Amer. Chem. Soc., Washington, D.C. (1981).
3. Palmer, S. R., Hippo, E. J., Kruge, M. A., and Crelling, J. C., In: Geochemistry of Sulfur in Fossil Fuels, W. L. Orr and C. M. White (eds.), ACS Symp. Series 429, ACS, Washington, DC (1990).
4. Gregg, S. J. and Sing, K. S. W., 1982. Adsorption, Surface Area and Porosity. Academic Press, New York, NY (1982).
5. Fuller, E. L., In: Coal Structure, M. L. Gorbaty and K. Ouchi (eds.), ACS 192, p. 293-309, American Chemical Society, Washington, D.C. (1981).
6. Marsh, H., Carbon 25, 49 (1987).
7. Sharkey, A. G. and McCartney, J. J., In: Chemistry of Coal Utilization, Second supplementary volume, M. A. Elliot (ed.), John Wiley & Sons, New York (1981).
8. Walker, P. L., Austin, L. G., and Nandi, S. P., Fuel 45, 173 (1966).
9. Kaji, R., Hishnuma, Y., and Nakamura, Y., Fuel, 64, 297 (1985).
10. Solomon, P. R., Hamblen, D. G., and Carengelo, R. M., In: Coal and Coal Products: Analytical Characterization Techniques, E. L. Fuller (ed.), ACS Symp. Series 205, ACS, Washington, DC (1982).
11. Painter, P. C., Sobkowiak, M., and Youtcheff, J., Fuel 66, 973 (1987).
12. Fuller, E. L., and Smyrl, M. R., Applied Spectroscopy 44, 451 (1990).
13. Smyrl, M. R. and Fuller, E. L., Jr., In: Coal and Coal Products: Analytical Characterization Techniques, E. L. Fuller (ed.), ACS Symp. Ser. 205, 133 (1982).
14. Clemens, A. H., Matheson, T. W., and Rogers, D. E., Fuel 70, 215 (1991).
15. Pisupati, S. V. and Scaroni, A. W., Fuel 72, 531 (1993).
16. Barret, E. P., Joyner, L. G. and Halenda, P. H., J. Amer. Chem. Soc. 73, 373 (1951).
17. Garrido, J., Linares-Solano, A., Martin-Martinez, J. M., Molina-Sabio, M., Rodriguez-Reinoso, F., and Torregrosa, R., Langmuir 3, 76 (1987).
18. Gan, H., Nandi, S. P., and Walker, P. L., Fuel 64, 272 (1972).
19. Mahajan, O. P., Carbon 29, 735 (1991).
20. Gumkowski, M., Liu, Q., and Arnett, E., Energy & Fuels 2, 295 (1988).
21. Machin, J. S., Staplin, F., and Deadmore, D. L., Illinois State Geological Survey Circ. 350, Champaign, IL (1963).
22. Thomas, J., and Damberger, H. H., 1976. Illinois State Geological Survey Circ., 493, Champaign, IL (1976).
23. Unsworth, J. F., Fowler, C. S., and Jones, L. F., Fuel 68, 18 (1989).
24. Nandi, S.P. and Walker, P.L., Jr., Separation Science 5, 441 (1976).
25. L'Homme, G. A., Pirard, J. P., and Ledent, P., In: Fundamental Issues in Control of Carbon Gasification Reactivity, J. Lahaye and P. Ehrburger (eds.), Kluwer Academic, Dordrecht, The Netherlands (1991).

**ACKNOWLEDGEMENTS:** This research was funded in part by the Illinois Department of Energy and Natural Resources through its Coal Development Board and Illinois Clean Coal Institute and by the U.S. Department of Energy. However, any opinions, findings, conclusions, or recommendations expressed herein are those of the authors and do not necessarily reflect the views of IDENR, ICCI, and DOE.

**Table 1. Analyses of eight IBCSP Coals.**

	IBC-101	IBC-102	IBC-103	IBC-105	IBC-106	IBC-107	IBC-108	IBC-109
Moisture (%)	14.7	14.2	5.7	9.4	10.4	9.3	45.0	9.2
Equil. moist (%,mmf)	16.0	15.8	6.7	16.2	11.9	16.7	-	10.8
Vol. matter (%,dmf)	44.4	41.8	38.8	43.4	42.5	44.4	42.5	37.6
Mineral matter (%,d)	13.6	9.3	10.7	22.6	11.8	14.5	5.9	9.6
Carbon (%, dmf)	80.1	81.7	83.4	82.1	81.5	79.6	80.6	82.8
Hydrogen (%,dmf)	6.0	5.9	5.6	5.9	5.6	5.7	5.6	5.4
Nitrogen (%, dmf)	1.5	1.6	1.9	1.6	1.9	1.4	1.6	1.9
Oxygen (%,dmf)	8.8	9.7	7.8	7.8	8.8	9.8	9.8	9.2
Sulfatic sulfur (%,d)	0.05	0.06	0.02	0.00	0.01	0.26	0.01	0.0
Pyritic sulfur (%,d)	1.2	2.2	1.1	2.5	1.8	0.8	0.4	0.5
Organic sulfur (%,dmf)	3.6	1.1	1.3	2.7	2.2	3.5	2.4	0.7
Total sulfur (%,d)	4.4	3.3	2.3	4.5	3.8	3.7	2.7	1.1
Chlorine (%,d)	0.12	0.02	0.18	0.10	0.02	0.08	0.03	0.42
BTU/lb (m,mmf)	12147	12537	13911	12334	13040	11779	-	13194
FSI	4.0	4.0	5.5	3.5	4.5	2.5	3.5	4.0
Rank	hVcb	hVcb	hVbb	hVcb	hVbb	hVcb	hVcb	hVb
Vitr. reflect.	0.46	0.62	0.74	0.50	0.54	0.56	0.58	0.73
Vitrinite (%,dmf)	88.3	89.9	85.7	86.7	85.7	86.6	89.6	87.4
Inertinite (%,dmf)	6.1	4.1	8.8	10.0	7.9	8.3	7.9	7.7
Liptinite (%,dmf)	5.6	6.0	5.5	3.3	6.4	5.1	2.6	4.9

**Table 2. Surface area and pore volume of fresh and oxidized IBCSP coals (-100 mesh), as measured with gas adsorption\*.**

Coal Sample	CO <sub>2</sub> surface area(m <sup>2</sup> /g)	N <sub>2</sub> surface area (m <sup>2</sup> /g)			N <sub>2</sub> pore volume (cc/g)**	
		Total	Mesopore	N <sub>2</sub> -Micropore	Total	Micropore
IBC-101	112 [135]	53 [45]	47 [42]	5.30 [3.85]	0.078 [0.071]	0.002 [0.002]
IBC-102	137 [139]	52 [44]	51 [43]	0.04 [1.14]	0.083 [0.071]	<0.001 [0.001]
IBC-103	148 [143]	4 [3]	4 [3]	0 [0]	0.017 [0.011]	0 [0]
IBC-105	116 [119]	21 [22]	18 [18]	2.73 [3.95]	0.032 [0.034]	0.001 [0.002]
IBC-106	134 [136]	27 [38]	24 [35]	1.84 [3.45]	0.040 [0.063]	0.001 [0.002]
IBC-107	120 [136]	43 [43]	39 [40]	3.85 [2.46]	0.063 [0.067]	0.002 [0.002]
IBC-108	143 [145]	16 [16]	16 [16]	0 [0]	0.026 [0.036]	0 [0]
IBC-109	152 [155]	14 [14]	13 [11]	1.69 [2.41]	0.024 [0.022]	0.001 [0.001]

\* Values in brackets are for oxidized coals.

\*\* For pores with diameters between about 5 Å and 1800 Å at a partial pressure of 0.99.

**Table 3. Surface area and pore volume of fresh and oxidized IBCSP coals (-100 mesh), as measured with mercury intrusion porosimeter\*.**

Coal Sample	Surface area (m <sup>2</sup> /g)			Pore volume(cm <sup>3</sup> /g)		
	30-500 Å pores	500-1800 Å pores	1800-10000 Å pores	30-500 Å pores	500-1800 Å pores	1800-10000 Å pores
IBC-101	94.2 [83.5]	0.5 [0.5]	0.4 [0.4]	0.16 [0.13]	0.01 [0.01]	0.05 [0.04]
IBC-102	91.9 [84.9]	0.7 [0.6]	0.5 [0.4]	0.16 [0.14]	0.01 [0.01]	0.06 [0.05]
IBC-103	60.5 [48.9]	0.3 [0.4]	0.4 [0.3]	0.09 [0.07]	0.01 [0.01]	0.05 [0.04]
IBC-105	58.9 [65.3]	0.4 [0.4]	0.3 [0.4]	0.09 [0.10]	0.01 [0.01]	0.05 [0.04]
IBC-106	38.6 [76.6]	0.4 [0.4]	0.3 [0.3]	0.07 [0.12]	0.01 [0.01]	0.04 [0.05]
IBC-107	83.8 [78.5]	0.5 [0.5]	0.4 [0.3]	0.13 [0.13]	0.01 [0.01]	0.03 [0.03]
IBC-108	65.7 [67.4]	1.1 [1.2]	2.4 [2.0]	0.10 [0.10]	0.03 [0.03]	0.34 [0.27]
IBC-109	80.7 [65.6]	0.4 [0.3]	0.3 [0.3]	0.12 [0.10]	0.01 [0.01]	0.04 [0.03]

\* Values in brackets are for oxidized coals.

**Table 4. Correlation coefficients for fresh -100 mesh IBCSP coals. Only correlations coefficients greater than 0.600 are included.\***

Carbon dioxide surface area-		Mercury surface area-	
volatile matter	-0.948	vitritinite content	0.794
vitritinite reflectance	0.940	inertinite content	-0.632
organic sulfur	-0.925		
BTU/lb	0.837	Mercury pore volume-	
nitrogen content	0.814	vitritinite content	0.908
equilibrium moisture	-0.825	inertinite content	-0.806
hydrogen content	-0.784		
carbon content	0.769		
mineral matter	-0.640		
nitrogen surface area	-0.610		
Nitrogen surface area-			
equilibrium moisture	0.891		
carbon content	-0.816		
BTU/lb	-0.789		
nitrogen content	-0.778		
inertinite content	-0.712		
vitritinite content	0.710		
mercury pore volume	0.710		
volatile matter	0.717		
hydrogen content	0.699		
oxygen content	0.655		
mercury surface area	0.644		
vitritinite reflectance	-0.626		
Nitrogen pore volume-			
equilibrium moisture	0.760		
inertinite content	-0.775		
mercury volume	0.761		
vitritinite content	0.752		
nitrogen content	-0.743		
BTU/lb	-0.717		
hydrogen content	0.703		
mercury surface area	0.668		
volatile matter	0.657		
oxygen content	-0.650		

\*Chemical and petrographic values are on a dry, mineral matter free (mmf) basis. Equilibrium moisture is on mmf basis. BTU/lb is on equilibrium moist, mmf basis.

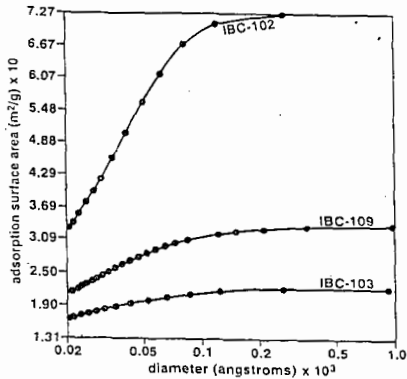


Figure 1. Cumulative surface area distribution in pores of various sizes for three of the fresh IBCSP coals as determined by the  $N_2$  gas adsorption method.

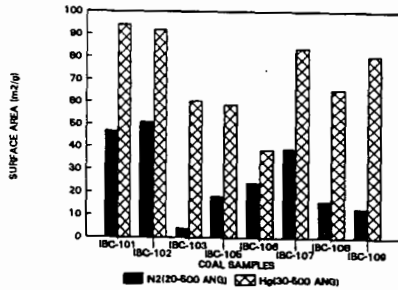


Figure 2. Comparison of surface areas of the IBCSP coals determined by  $N_2$  adsorption and mercury intrusion methods.

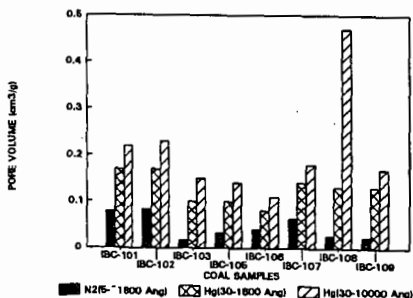


Figure 3. Comparison of pore volumes of the IBCSP coals determined by  $N_2$  adsorption and mercury intrusion

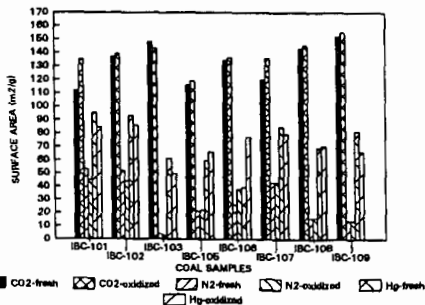


Figure 4. Effect of oxidation on the surface area of eight IBCSP coals.

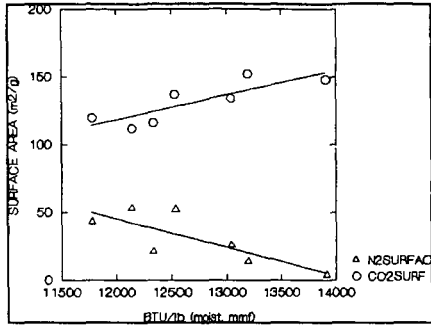


Figure 5. Variation of CO<sub>2</sub> and N<sub>2</sub> surface areas with heating value (BTU/lb) of fresh IBCSP coals.

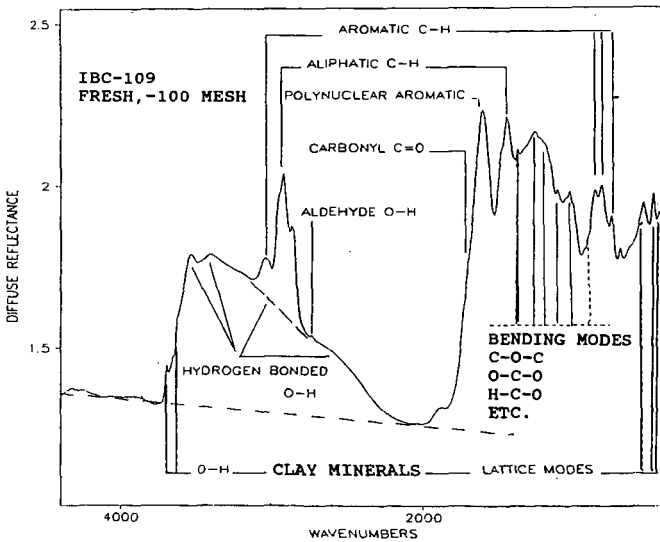


Figure 6. DRIS spectrum of fresh -100 mesh IBC-109 coal.

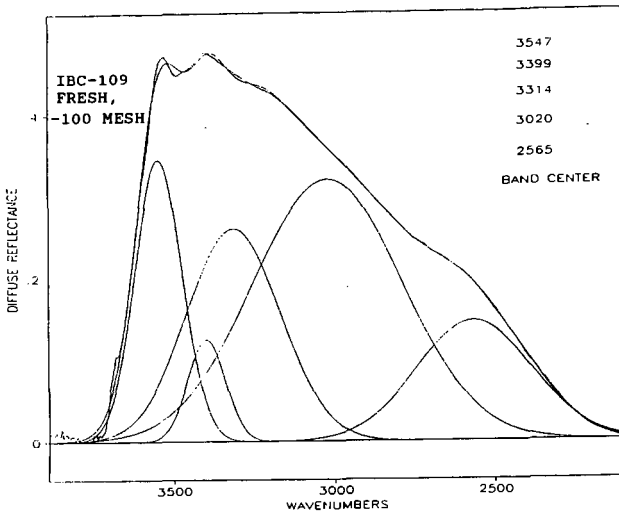


Figure 7. Deconvolution of hydroxyl band envelope of Figure 6 into its constituent components. Chi-squared of summation curve relative to parent curve=0.0204.

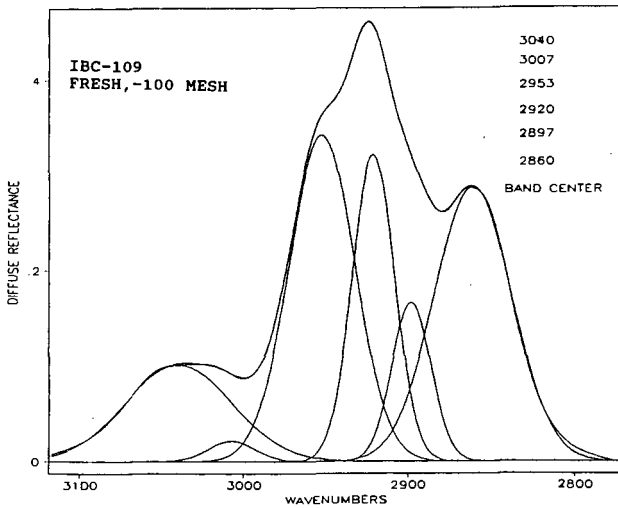


Figure 8. Deconvolution of hydrocarbon band envelope of Figure 8 into its constituent components. Chi-squared of summation curve relative to parent curve=0.000738.

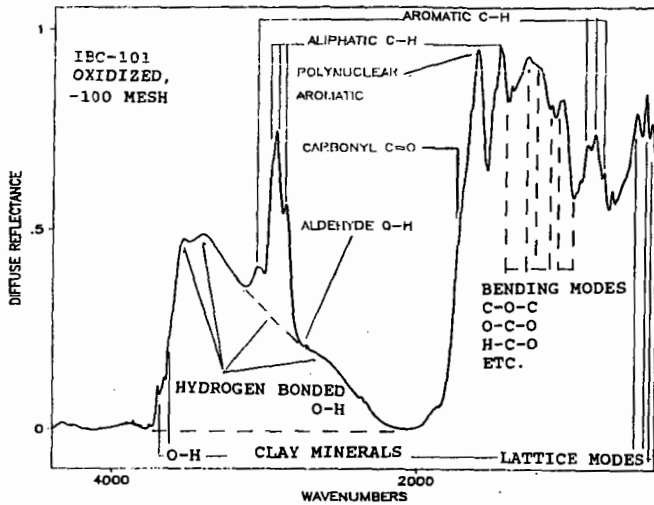


Figure 9. DRIS spectrum of oxidized -100 mesh IBC-101 coal.

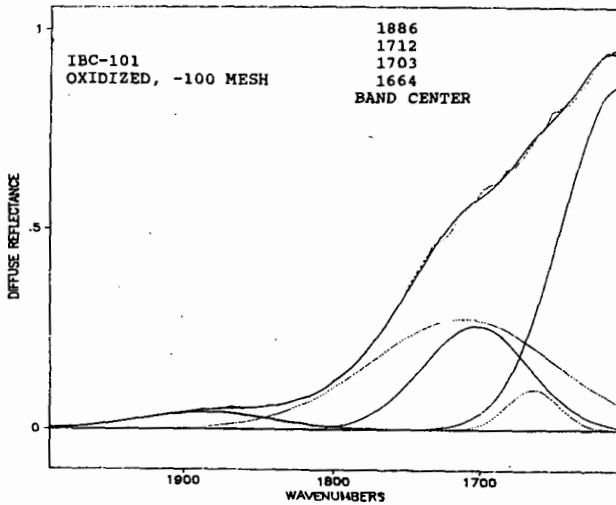


Figure 10. Band deconvolution for carbonyl region of the DRIS spectrum of the oxidized -100 mesh IBC-101 coal.